Engineering Failure Analysis 110 (2020) 104361

Contents lists available at ScienceDirect

Engineering Failure Analysis

journal homepage: www.elsevier.com/locate/engfailanal

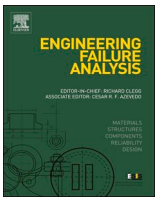

Rapid strain energy density evaluation for V-notches under mode I loading conditions

Pietro Foti[a,*], Majid R. Ayatollahi[b], Filippo Berto[a]

[a] Norwegian University of Science and Technology, MTP Gløshaugen, Richard Birkelands vei 2B, Trondheim 7491, Norway
[b] School of Mechanical Engineering, Iran University of Science and Technology, Narmak, Tehran, Iran

ARTICLE INFO

Keywords:
Strain energy density method
Finite element analysis
Control volume
Correcting formula
Free coarse mesh

ABSTRACT

This work investigates the possibility to evaluate the Strain Energy Density value with a free mesh model suggesting the use of a correcting formula a posteriori.

Several numerical analyses were carried out to prove the good agreement between the method suggested and the conventional method considered until now to acquire the Strain Energy Density value that requires the construction of the so-called control volume in the pre-processing phase of the FEM code.

The main advantage of the methodology shown in the present work to evaluate the Strain Energy Density value is that, accepting an error in the calculation that depends on different parameters, it is possible to apply this method directly as a post-processing tool.

This allows also to decrease considerably the effort of the researcher in applying this method and to reduce the calculation time thanks to the use of a free coarse mesh.

1. Introduction

The presence of a notch or, in a more general term, of a geometrical discontinuity in a component determines the presence of a localised stress concentration; this could generate a crack affecting considerably the strength and the assessed fatigue life of such a component.

Since it is impossible to avoid the presence of intrinsic defects in mechanical components and of geometrical discontinuities, it is particularly important to have specific and reliable tools to assess the structural integrity and the expected fatigue life of the components analysed.

The scientific discipline that studies the prevention of fractures is called fracture mechanics; however, even if the field of fracture mechanics is a topic of active and continuous research, still nowadays the matter of fracture of materials under different loading conditions is far than completely solved.

The problem of brittle fracture can be treated applying a huge variety of methods [1–3] whose practical application, however, is possible only neglecting some aspects of the problem analysed; indeed it is not always possible to take into account all the parameters that could affect the fracture process because of lack of experimental data, limitations of the method considered or also because, even if software are often used to get more accurate results, the computational time needed could result to be too high for the accuracy required.

This means that the use of these methods depends on the aspect of the problem of more interest for the researcher or on the aspects that affect more the fracture process analysed in order to get reliable results in reasonable time. This make clear that the

* Corresponding author.
E-mail address: pietro.foti@ntnu.no (P. Foti).

https://doi.org/10.1016/j.engfailanal.2019.104361
Received 3 September 2019; Received in revised form 22 December 2019; Accepted 30 December 2019
Available online 07 January 2020

Nomenclature

A	Control volume area in 2D problems.
A′	Approximated control volume area achieved through the FE analysis
E	Young's modulus
e_1, e_2, e_3	mode 1, 2 and 3 functions of 2α in the SED expressions for sharp V-notches
I_1, I_2	mode 1 and 2 functions in the SED expression for sharp V-notches. Assessed as:$I_{1(\gamma)} = \int_{-\gamma}^{+\gamma} f_1(\theta)d\theta$;$I_{2(\gamma)} = \int_{-\gamma}^{+\gamma} f_2(\theta)d\theta$
K_{IC}	fracture toughness
K_1^N, K_2^N	mode I and II notch stress intensity factors of a sharp V-notch. Assessed as: $K_1^N = \sqrt{2\pi}\lim_{r\to 0^+} r^{1-\lambda_1}\sigma_{\theta\theta}(r,\ \theta = 0)$; $K_2^N = \sqrt{2\pi}\lim_{r\to 0^+} r^{1-\lambda_2}\sigma_{r\theta}(r,\ \theta = 0)$.
r, θ	polar coordinates
R_0	control volume radius
SED	strain energy density
$\bar{W}$	averaged strain energy density
W_C	critical strain energy

Greek

2α	opening angle of V-notch
γ	supplementary angle of α:$\gamma = \pi - \alpha$
$\Delta\sigma_a$	fatigue strength of the butt ground welded joints
ΔK_{1A}^N	NSIF-based fatigue strength of welded joints
ΔW_L	critical value of the mean SED that corresponds to the fatigue limit
λ_1, λ_2	mode 1 and 2 Williams' eigenvalues for stress distribution at V-notches
ν	Poisson's ratio
σ_t	ultimate tensile strength
σ_{ij}	ij component of the stress tensor
$\widetilde{\sigma}_{ij}$	angular stress functions
$\sigma_{\theta\theta}$, σ_{rr}, $\tau_{r\theta}$	stresses in the polar coordinate system
χ_1, χ_2	auxiliary parameters, function of opening angle

application of a method with respect to another is determined mostly on what the research or the designer are looking for but also on their expertise and on the tools available; indeed, it is also important to say that each method developed to deal with fracture follows its own methodology.

Among the methods available to deal with brittle failure, we focus in this work on the Strain Energy Density (SED) method, an energetic local approach validated as a method to investigate both fracture in static condition and fatigue failure [4–11] dealing with both sharp-V [12–19] and blunt V- and U-notches [20–27].

The basic idea of this method is that the brittle fracture occurs when the local SED W, evaluated in a given control volume, reaches a critical value $\bar{W} = W_C$, independent of the notch opening angle and of the loading type [4,28], that is evaluable, in the case of an ideally brittle material, through the following expression:

$$W_C = \frac{\sigma_t^2}{2E} \tag{1}$$

Being σ_t the conventional ultimate tensile strength and E the Young's modulus.

Even if this methods based on a very simple concept, it requires expertise in its application due to the peculiarity of the mesh required for the finite elements model; indeed its application needs a FE model built in order to have the control volume centered on the critical point of the component analysed according to the theory of the method that is explained in Section 2.1.

The main aim of the present work is to provide numerical data to make the SED method more suitable for its practical application also as a post-processing tool to be integrated in the most known commercial software to investigate structural integrity and fatigue resistance.

This can be also helpful in topology optimisation techniques [29,30]. Indeed, without the need of a mapped mesh, the SED method is more suitable to be used also with this kind of techniques that could beneficiate of all the advantages leaded by this method from the mesh low sensitivity to the possibility to take into account mixed mode loading and considering both structural integrity and fatigue strength. We should underline that, usually, a topology optimised component is produced through additive manufacturing techniques due to the complex forms that naturally occurred during the topology optimisation. Anyway, in some recent works, the SED method has been applied also to additive manufactured components showing very good results [19,27].

In order to simplify the method, we evaluated in this work the possibility to estimate the value of the SED without the construction of the control volume in the pre-processing phase of the FEM code suggesting also a correcting formula to decrease the error of the value achieved.

2. Materials and method

2.1. Strain energy density analytical frame

In this section we explain the principal equations of the SED method in order to make the reader understand the considerations about the correcting formula suggested and its range of validity.

Assuming valid for the material analysed the hypothesis of linear elastic isotropic material [4,5], the total strain energy density is given by the following expression:

$$W(r,\theta)=\frac{1}{2E}\{\sigma_{11}^2+\sigma_{22}^2+\sigma_{33}^2-2\nu(\sigma_{11}\sigma_{22}+\sigma_{11}\sigma_{33}+\sigma_{22}\sigma_{33})+2(1+\nu)\sigma_{12}^2\} \tag{2}$$

Dealing with V-notches, taking into account Williams' equations under the hypothesis of plane stress or plane strain conditions, the stress field [31] near the notch tip is described by Eq. (3) for mode I loading and by Eq. (4) for mode II loading according to the polar coordinate system (r,θ) shown in Fig. 1.

$$\begin{Bmatrix}\sigma_{\theta\theta}\\ \sigma_{rr}\\ \tau_{r\theta}\end{Bmatrix}_{\rho=0}=\frac{1}{\sqrt{2\pi}}\frac{r^{\lambda_1-1}K_1^N}{(1+\lambda_1)+\chi_1(1-\lambda_1)}\left[\begin{Bmatrix}(1+\lambda_1)\cos(1-\lambda_1)\theta\\ (3-\lambda_1)\cos(1-\lambda_1)\theta\\ (1-\lambda_1)\sin(1-\lambda_1)\theta\end{Bmatrix}+\chi_1(1-\lambda_1)\begin{Bmatrix}\cos(1+\lambda_1)\theta\\ -\cos(1+\lambda_1)\theta\\ \sin(1+\lambda_1)\theta\end{Bmatrix}\right] \tag{3}$$

$$\begin{Bmatrix}\sigma_{\theta\theta}\\ \sigma_{rr}\\ \tau_{r\theta}\end{Bmatrix}_{\rho=0}=\frac{1}{\sqrt{2\pi}}\frac{r^{\lambda_2-1}K_2^N}{(1-\lambda_2)+\chi_2(1+\lambda_2)}\left[\begin{Bmatrix}-(1+\lambda_2)\sin(1-\lambda_2)\theta\\ -(3-\lambda_2)\sin(1-\lambda_2)\theta\\ (1-\lambda_2)\cos(1-\lambda_2)\theta\end{Bmatrix}+\chi_2(1+\lambda_2)\begin{Bmatrix}-\sin(1+\lambda_2)\theta\\ \sin(1+\lambda_2)\theta\\ \cos(1+\lambda_2)\theta\end{Bmatrix}\right] \tag{4}$$

K_1 and K_2 being the Notch stress intensity factors (NSIFs) related to mode I and mode II stress distributions [32].

Introducing $\tilde{\sigma}_{\theta\theta}$, $\tilde{\sigma}_{rr}$and $\tilde{\sigma}_{r\theta}$, function of the notch opening angle 2α and of the position with the polar coordinate θ, the stress field close to the notch tip in a mixed mode loading (I + II) can be expressed as follows exploiting the superposition principle:

$$\begin{Bmatrix}\sigma_{\theta\theta}\\ \sigma_{rr}\\ \tau_{r\theta}\end{Bmatrix}_{\rho=0}=r^{\lambda_1-1}\cdot K_1\cdot\begin{vmatrix}\tilde{\sigma}_{\theta\theta}^{(1)} & \tilde{\sigma}_{r\theta}^{(1)} & 0\\ \tilde{\sigma}_{r\theta}^{(1)} & \tilde{\sigma}_{rr}^{(1)} & 0\\ 0 & 0 & \tilde{\sigma}_{zz}^{(1)}\end{vmatrix}+r^{\lambda_2-1}\cdot K_2^N\cdot\begin{vmatrix}\tilde{\sigma}_{\theta\theta}^{(2)} & \tilde{\sigma}_{r\theta}^{(2)} & 0\\ \tilde{\sigma}_{r\theta}^{(2)} & \tilde{\sigma}_{rr}^{(2)} & 0\\ 0 & 0 & \tilde{\sigma}_{zz}^{(2)}\end{vmatrix} \tag{5}$$

In mixed-mode loading conditions, the SED value around the notch tip is given by three different contributions:

$$W(r,\theta)=W_1(r,\theta)+W_2(r,\theta)+W_{12}(r,\theta)$$

Being:

$$W_1(r,\theta)=\frac{1}{2E}\cdot r^{2(\lambda_1-1)}\cdot(K_1)^2[\tilde{\sigma}_{\theta\theta}^{(1)^2}+\tilde{\sigma}_{rr}^{(1)^2}+\tilde{\sigma}_{zz}^{(1)^2}-2\nu(\tilde{\sigma}_{\theta\theta}^{(1)}\tilde{\sigma}_{rr}^{(1)}+\tilde{\sigma}_{\theta\theta}^{(1)}\tilde{\sigma}_{zz}^{(1)}+\tilde{\sigma}_{zz}^{(1)}\tilde{\sigma}_{rr}^{(1)})+2(1+\nu)\tilde{\sigma}_{r\theta}^{(1)^2}] \tag{7}$$

$$W_2(r,\theta)=\frac{1}{2E}\cdot r^{2(\lambda_2-1)}\cdot(K_2)^2[\tilde{\sigma}_{\theta\theta}^{(2)^2}+\tilde{\sigma}_{rr}^{(2)^2}+\tilde{\sigma}_{zz}^{(2)^2}-2\nu(\tilde{\sigma}_{\theta\theta}^{(2)}\tilde{\sigma}_{rr}^{(2)}+\tilde{\sigma}_{\theta\theta}^{(2)}\tilde{\sigma}_{zz}^{(2)}+\tilde{\sigma}_{zz}^{(2)}\tilde{\sigma}_{rr}^{(2)})+2(1+\nu)\tilde{\sigma}_{r\theta}^{(2)^2} \tag{8}$$

$$W_{12}(r,\theta)=\frac{1}{E}\cdot r^{\lambda_1+\lambda_2-2}\cdot K_1\cdot K_2[\tilde{\sigma}_{\theta\theta}^{(1)}\tilde{\sigma}_{\theta\theta}^{(2)}+\tilde{\sigma}_{rr}^{(1)}\tilde{\sigma}_{rr}^{(2)}+\tilde{\sigma}_{zz}^{(1)}\tilde{\sigma}_{zz}^{(2)}-\nu(\tilde{\sigma}_{\theta\theta}^{(1)}\tilde{\sigma}_{rr}^{(2)}+\tilde{\sigma}_{\theta\theta}^{(1)}\tilde{\sigma}_{zz}^{(2)}+\tilde{\sigma}_{zz}^{(1)}\tilde{\sigma}_{rr}^{(2)}+\tilde{\sigma}_{\theta\theta}^{(2)}\tilde{\sigma}_{rr}^{(1)}+\tilde{\sigma}_{\theta\theta}^{(2)}\tilde{\sigma}_{zz}^{(1)}+\tilde{\sigma}_{zz}^{(2)}\tilde{\sigma}_{rr}^{(1)})+2(1+\nu)\tilde{\sigma}_{r\theta}^{(1)}\tilde{\sigma}_{r\theta}^{(2)}] \tag{9}$$

Being W_1 the contribute of mode I loading acting alone, W_2 the contribute of mode II loading acting alone whileW_{12} is a combined contribute of both the two modes to be considered only when they act together.

In order to evaluate the averaged value of the strain energy density, a sector-shaped cylinder of radius R_0 along the notch tip line, called 'control volume', is considered. For more consideration about the shape of the control volume, we remand to Refs. [1,8,33] In plane problems, both in mode I and mixed mode (I + II) loading, the control volume becomes a circle or a circular sector with radius R_0 respectively in the case of cracks and pointed V-notches, as shown in Fig. 2.

In both the cases of the crack and of a V-notch, the radius R_0 can be estimated both under plane strain [34–36] and plane stress [14].

Integrating the strain energy density in the control volume considered, it is possible to get the elastic deformation energy around the notch tip as follows:

$$E_{(R)}=\int_A W\cdot dA=\int_0^R\int_{-\gamma}^{+\gamma}[W_1(r,\theta)+W_2(r,\theta)+W_{12}(r,\theta)]\cdot r dr d\theta \tag{10}$$

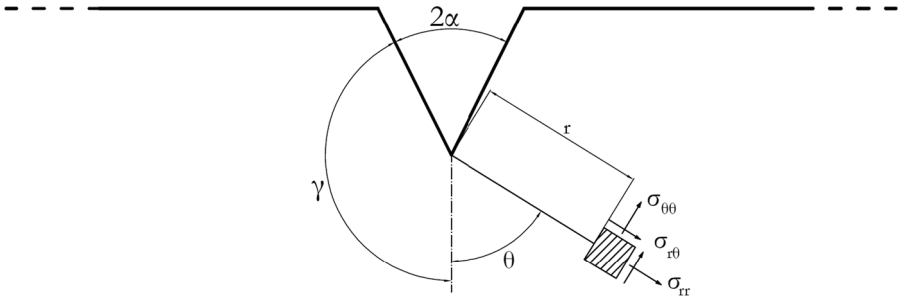

Fig. 1. Coordinate system and symbols used for the stress field components.

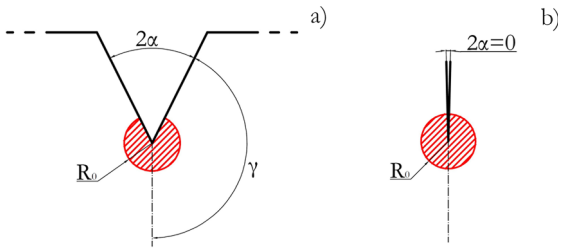

Fig. 2. Control volume (area) for. (a) Sharp V-notch; (b) crack.

Being the contribution of W_{12} equals to zero because of the symmetry of the integration field, the elastic deformation energy is given by:

$$E_{(R)} = E_{1(R)} + E_{2(R)} = \frac{1}{E}\cdot\frac{I_{1(\gamma)}}{4\lambda_1}\cdot(K_1)^2\cdot R^{2\lambda_1} + \frac{1}{E}\cdot\frac{I_{2(\gamma)}}{4\lambda_2}\cdot(K_2)^2\cdot R^{2\lambda_2} \tag{11}$$

Beingλ and I_1, available in the literature, dependent on α and on the stresses field. In 2D problems, the value of the area on which the integration is carried out is given by:

$$A_{(R)} = \int_0^{R_0}\int_{-\gamma}^{+\gamma} r dr d\theta = R_0^2\gamma \tag{12}$$

γ being expressed in radians. Considering Eqs. (11) and (12), the averaged elastic deformation energy on the area results to be:

$$\bar{W} = \frac{E_{(R)}}{A_{(R)}} = \frac{1}{E}\cdot\frac{I_{1(\gamma)}}{4\lambda_1\gamma}\cdot(K_1)^2\cdot R_0^{2(\lambda_1-1)} + \frac{1}{E}\cdot\frac{I_{2(\gamma)}}{4\lambda_2\gamma}\cdot(K_2)^2\cdot R_0^{2(\lambda_2-1)} = \frac{1}{E}\cdot e_{1(2\alpha)}\cdot(K_1)^2\cdot R_0^{2(\lambda_1-1)} + \frac{1}{E}\cdot e_{2(2\alpha)}\cdot(K_2)^2\cdot R_0^{2(\lambda_2-1)} \tag{13}$$

Taking into account all the three modes of loading, I + II + III, [14] the value of the strain energy density is given by:

$$\bar{W} = \frac{e_1}{E}\left[\frac{K_1}{R_0^{1-\lambda_1}}\right]^2 + \frac{e_2}{E}\left[\frac{K_2}{R_0^{1-\lambda_2}}\right]^2 + \frac{e_3}{E}\left[\frac{K_3}{R_0^{1-\lambda_3}}\right]^2 \tag{14}$$

2.2. Rapid strain energy density evaluation

The SED low mesh sensibility has already been hugely proved [37–41]. However, the numerical data already available in literature has been obtained with FE models that involved the construction of the control volume in the pre-processing phase of the FE analysis. In the present work we are going to show that a good estimation of the SED value is possible also with a completely free mesh.

Dealing with V-notch in plane condition, the control volume area is given by Eq. (12) while the Strain Energy Density value can be estimated from Eq. (13).

Considering the Eq. (13) limited to mode I loading conditions and comparing it with Eq. (12) it is possible to state that:

$$\bar{W} = \frac{1}{E}\cdot e_{1(2\alpha)}\cdot(K_1)^2\cdot R_0^{2(\lambda_1-1)} \propto (\gamma\cdot R_0^2)^{\lambda_1-1} \tag{15}$$

We can state that:

$$\bar{W} = \left(\frac{e_{1(2\alpha)}}{E\cdot\gamma^{\lambda_1-1}}\cdot K_1^2\right)\cdot A^{\lambda_1-1} \tag{16}$$

Applying the logarithmic operator, we have that:

$$\log(\bar{W}) = \log\left(\frac{e_{1(2\alpha)}}{E\cdot\gamma^{\lambda_1-1}}\cdot K_1^2\right) + (\lambda_1-1)\cdot\log(A) \tag{17}$$

This means that in a double logarithmic diagram the trend of the SED value with varying the volume is described by a straight line with a slope equal to $(\lambda_1 - 1)$. Being the mode I singular with notch opening angle less than 180°, the slope of the straight line is negative.

With some easy passages it is possible to get the following equation:

$$\bar{W}_{R_0} = \bar{W}_{A'}\cdot\left(\frac{\gamma R_0^2}{A'}\right)^{\lambda_1-1} \tag{18}$$

Being $\bar{W}_{A'}$the SED value for a control volume with an area equal to A'.

This means that the strain energy density value does not need to be evaluated in a control volume with a radius equal to R_0. However, some considerations must be done:

- The shape of the control volume has to be that of a circular sector. Indeed, the considerations done in the present paragraph are valid only in the case of a circular sector-shaped control volume. Only in this case it is possible to evaluate the SED value according to Eq. (13) that represent actually the starting point to achieve the correcting formula reported in Eq. (18).
- The control volume radius has to be within a distance from the notch tip that ensure the prevalence of the local effect of the notch tip on the stress field. A control volume, obtained through a polar selection with a radius too much big, could result in an overestimation of the SED value evaluated through the Eq. (18).

From the numerical data acquired, the authors also noticed that without using the correcting formula reported above a good evaluation of the SED value is already possible with a mesh size of 1/8 of the control volume radius almost independently on the value of the control volume radius. This, according to the present authors, should be referred to the fact that, expressing the mesh size as a ratio of the control volume radius, the shape of a circular-sector is approximated almost with the same error being the ratio between the mesh size and the control volume radius the same. This confirms that the error gained is mostly due to the approximation of the circular sector shape but does not exclude that a good approximation of the SED value can be acquired without the construction of the control volume in the pre-processing phase of the FE analysis.

2.3. FE analysis

In order to verify the correcting formula suggested in the Section 2.2 coupled with the possibility to use a control volume free model, we carried out a series of FE analysis considering the simple case of a sharp V-notched specimen, shown in Fig. 3 with its geometrical parameters. As regard the notch opening angle 2α, in order to verify the exponent of the correcting formula suggested, three different cases were considered $2\alpha = |90°;120°;135°|$.As regards the control volume radius, it varies, with regards to the notch depth, as: R_0/a = [0.028; 0.042; 0.084; 0.126; 0.168; 0.210; 0.252; 0.294; 0.315]. Different cases are taken into account to verify the exponent of the correcting formula suggested and to prove that, however, there is a limitation, in terms of radius of the control volume considered, to a distance that ensure the prevalence of the local effect of the notch tip on the stress field. The mesh refinement varies as ratio of the control volume radius between [] [1/4; a1/6; a1/8; a1/10; a1/100] for a total of 5 different cases.

Four different models, shown in Fig. 4, are considered.

The model A, showed in Fig. 4(a), results to be the conventional FE model built to evaluate the SED value with the construction of the control volume. The model B, shown in Fig. 4(b), has the control volume built in the pre-processing phase of the FE analysis, but it considers a free mesh. In the model C, shown in Fig. 4(c), it was used a mapped mesh, but the model does not have a control volume. In this case a mapped mesh was considered to take into account those FE models built for any other purpose by designers or researchers in order to estimate the error in the evaluation of the SED value as a post-processing tool. The model D, shown in Fig. 4(d), considers instead a completely free mesh with only a refinement in the notch tip in order to consider the error in the evaluation of the SED value considering the easiest way possible to build the model.

In order to acquire the SED value, as regard the models A and B, it was considered the conventional procedure used to apply the SED method as it is possible to see from Fig. 5(a) and (b), while, as regards the models C and D, the SED value is acquired through a selection of the elements close to the notch tips using a polar coordinate system centered in the notch tip with a radius equals to the

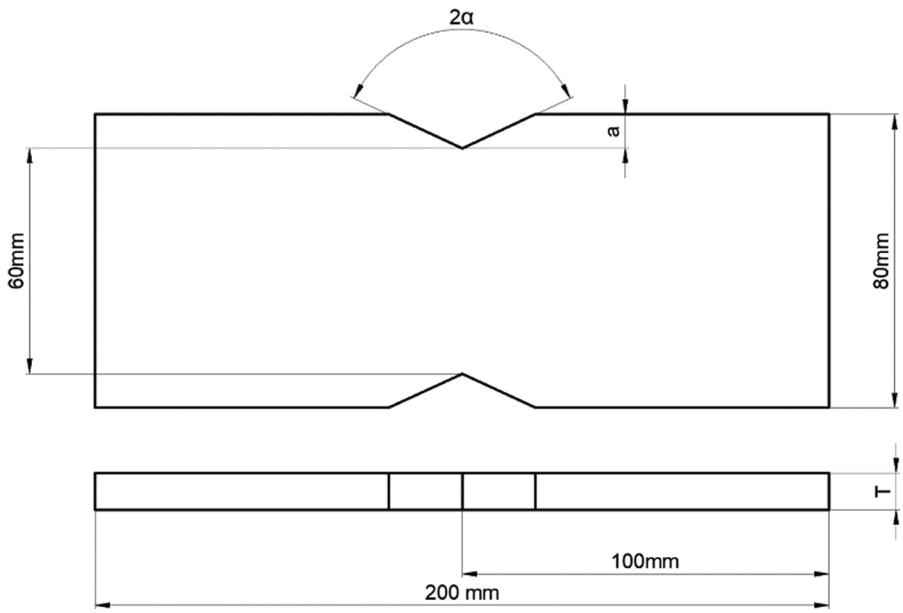

Fig. 3. Geometry analysed.

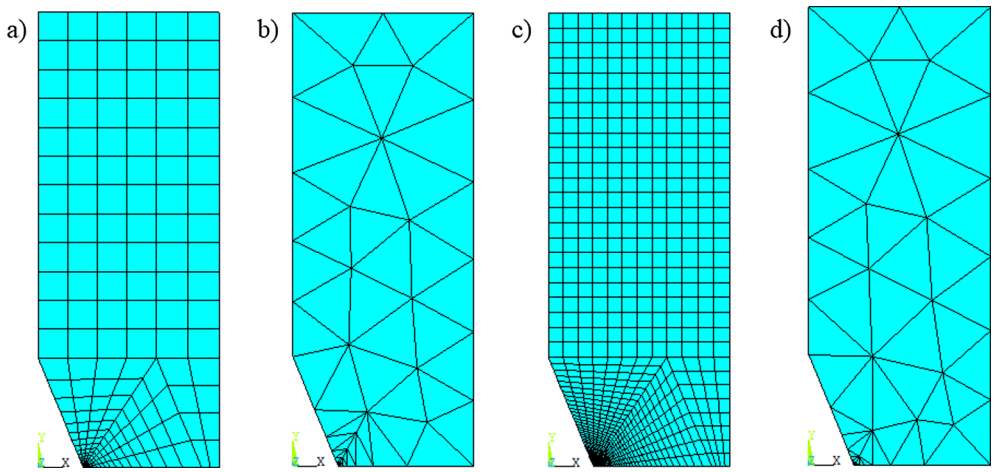

Fig. 4. FE models for: (a) mapped mesh with control volume, model A; (b) free mesh with control volume, model B; (c) mapped mesh without control volume, model C; (d) free mesh without control volume, model D.

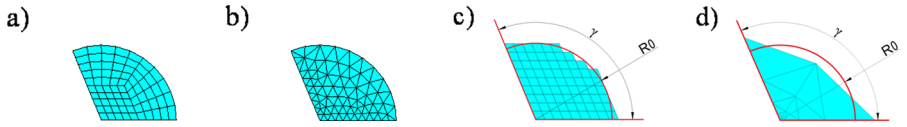

Fig. 5. Control volume for: (a) mapped mesh with control volume; (b) free mesh with control volume; (c) mapped mesh without control volume; (d) free mesh without control volume.

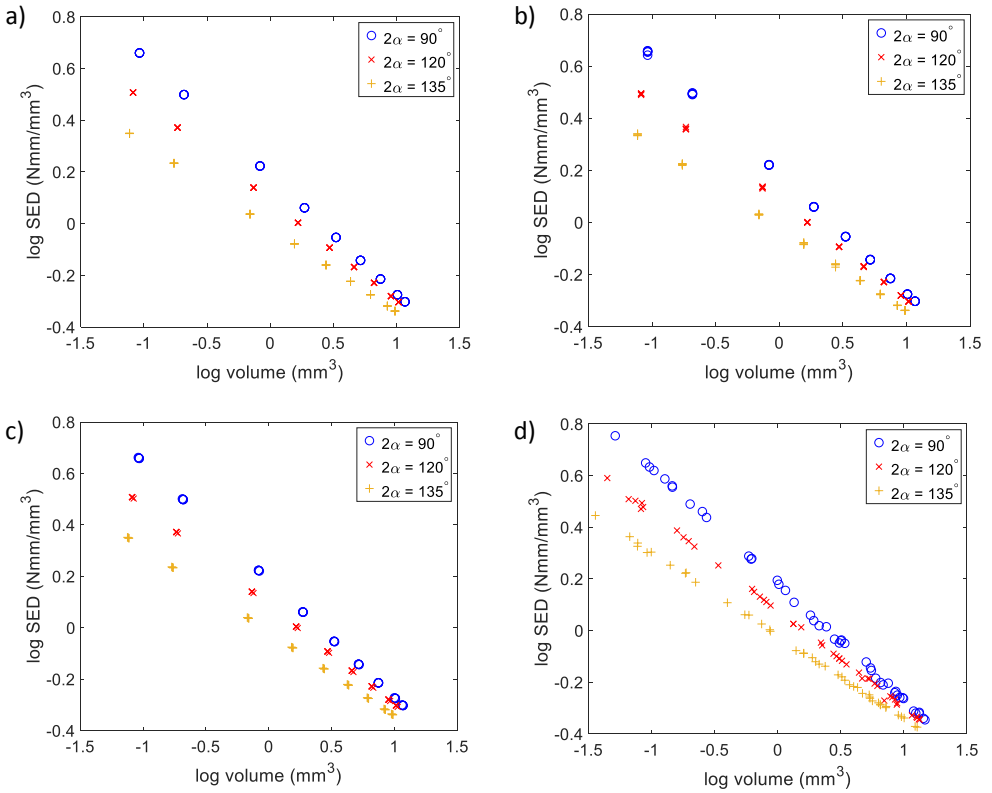

Fig. 6. SED vs volume trends for: (a) mapped mesh with control volume; (b) free mesh with control volume; (c) mapped mesh without control volume; (d) free mesh without control volume.

control volume radius considered. The result of such a selection is shown both in Fig. 5(c) for a mapped mesh and in Fig. 5(d) for a completely free mesh.

3. Results and discussion

As stated above, the main aim of the present work is to suggest a correcting formula that allows the use of a free mesh to evaluate the SED value. In order to prove the validity of the formula suggested in Section 2.2 we report in Fig. 6 the trend of the SED value with varying the control volume. Table 1 reports the value of λ found interpolating the data reported in Fig. 6 for the three different opening angles and the four different models considered in the present work.

In Fig. 7, analysing the results reported in Fig. 6(d) for a notch opening angle of 90° (the same considerations are possible also with the other angles), distinguishing the different data acquired with different mesh refinements but using the same value of the radius to carry out the selection with polar coordinates. It is possible to notice that, using the methodology suggested in the present work, the approximation in evaluating the control volume area it is, of course, different considering different mesh refinements but also that the error, in evaluating the theoretical value of the control volume area for a particular radius, is in part compensated by the error in evaluating the SED value; this is the reason why the present authors, in suggesting a correcting formula, prefer the use of the control volume area found directly with the selection of the elements instead of the theoretical one that could be evaluated through the value of the radius chosen to carry out the selection with polar coordinates.

In Fig. 8, for each case of opening angle, control volume and mesh refinement considered, it is reported the error in evaluating the

Table 1
Williams eigenvalues found interpolating the numerical data acquired.

Opening Angle	Williams' eigenvalue								
	Theoretical value	Model A		Model B		Model C		Model D	
		Value	Δ%	Value	Δ%	Value	Δ%	Value	Δ%
90°	0.5448	0.5420	−0.51	0.5448	0.00	0.5421	−0.50	0.5496	0.88
120°	0.6157	0.6144	−0.21	0.6212	0.89	0.6144	−0.21	0.6233	1.23
135°	0.6736	0.6732	−0.06	0.6794	0.86	0.6733	−0.04	0.6776	0.59

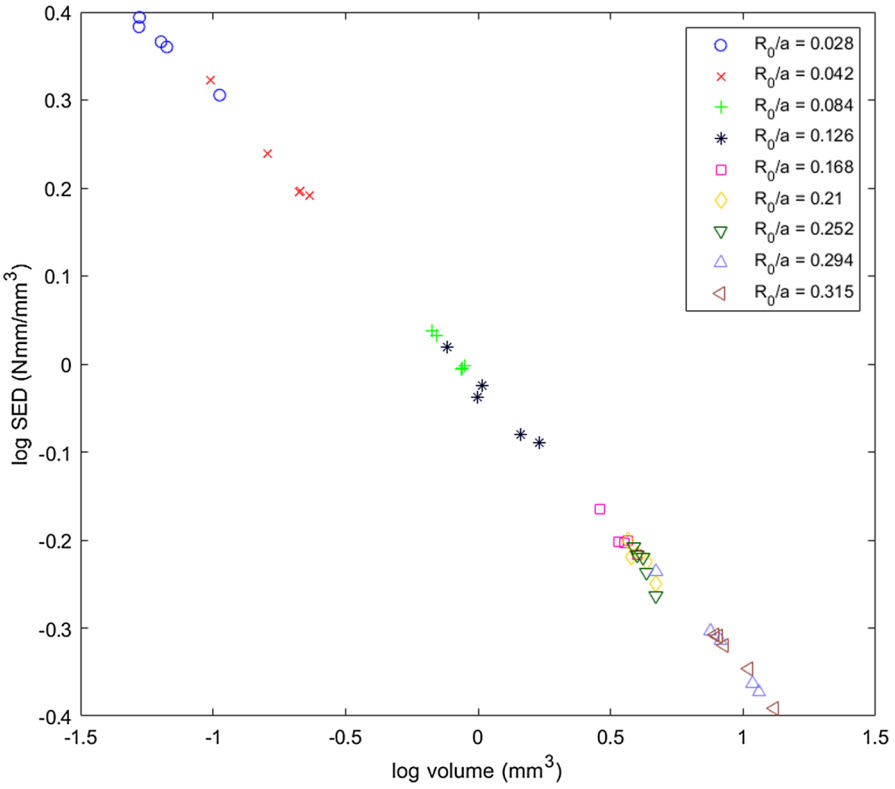

Fig. 7. SED vs volume trends for free mesh without control volume.

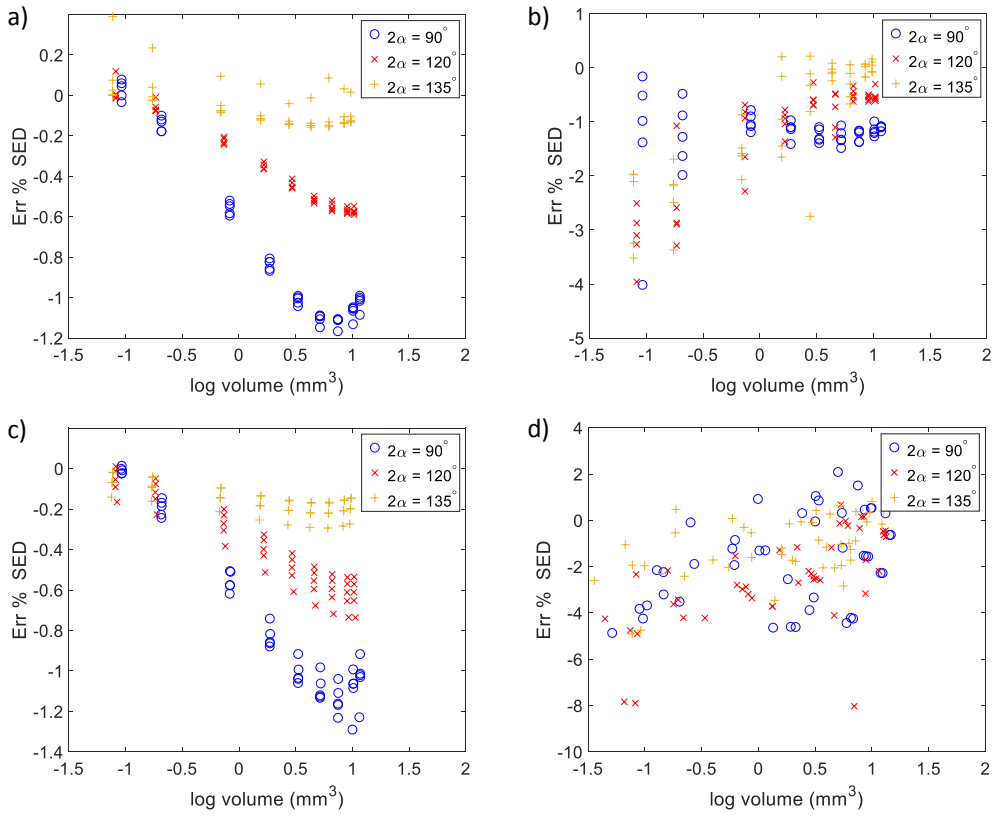

Fig. 8. Error acquired using the correcting formula suggested for: (a) mapped mesh with control volume; (b) free mesh with control volume; (c) mapped mesh without control volume; (d) free mesh without control volume.

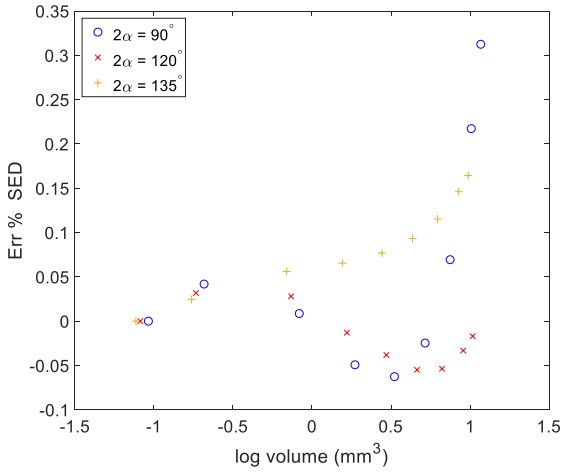

Fig. 9. Error acquired using the correcting formula suggested for the model with mapped mesh and control volume.

SED value achieved exploiting the correcting formula reported in Eq. (18) using as reference case the value acquired with the numerical analysis carried out with the most refined mesh with the model A and considering a control volume radius that gives a ratio with the notch depth equals to 0.028.

Comparing Fig. 8(a) and (c) with Fig. 8(b) and (d), it is possible to see that, as regards the models with a mapped mesh, the error follows a trend while, as regards the models with a free mesh, the error is stochastic. According to the authors this should be referred to how the mapped mesh utilised is built. Indeed, even if the control volume radius and the mesh refinement change, the model is built always in the same way and it is also similar for both the models A and C. This is also clear comparing the value of λ found interpolating the numerical data for these two models reported in Table 1.

Table 2
Williams eigenvalues found interpolating the numerical data acquired for the first three values of the control volume radius with the model A.

Notch opening angle	Williams' eigenvalue
90°	0.5418
120°	0.6146
135°	0.6730

From Fig. 8(a) and (c), in particular for the case of 90°, it is possible to notice how the error start to increase after a certain value of the volume; this is due to the fact that for radius major than a limit value the stress field can no longer be described by William's equations resulting in an overestimation of the SED value.

To make more clear this last consideration we applied the correcting formula, suggested in Section 2.2, using, as Williams' eigenvalue, the value obtained interpolating the numerical data for the first three values of the control volume radius, reported in Table 2, in order to be sure that the stress field can be still considered described by Williams' equations and to neglect any possible error related to the bad estimation of lambda caused from the mapped mesh and the geometrical parameters chosen for the model.

Fig. 9 shows the error, for the model A, obtained using the value of Williams' eigenvalue reported in Table 2:

From Fig. 9. it is possible to see that after a certain value of the control volume radius the error increase because the stress field does not follow anymore Williams' equations.

The authors suggest considering a limit ratio of 0.2 between the radius chosen to carry out the selection and the notch depth.

4. Conclusions

The main aim of the paper was to provide enough numerical data to prove the possibility to evaluate the SED value with a free coarse mesh though the exploitation of a correcting formula.

The numerical analysis carried out showed that:

- A good estimation of the SED value is possible with a free coarse mesh.
- The SED value can be evaluated also with different control volume radius thanks to the possibility to correct the value acquired with the formula suggested in the present work.
- The control volume considered must be within a distance from the notch tip that ensure the prevalence of the local effect of the notch tip on the stress field.
- The SED value for a small radius, evaluated considering the value obtained with a control volume radius too much big and applying the correcting formula suggested, is overestimated.
- The error in evaluating the SED value is mostly due to the approximation of the theoretical shape of the control volume.
- A good estimation of the SED value is possible with a mesh size of 1/8 of the control volume radius near the notch tip; indeed, this mesh size guarantees a good approximation of the theoretical shape of the control volume and therefore, for what stated above, a good estimation of the SED value.

Declaration of Competing Interest

The authors declare that they have no known competing financial interests or personal relationships that could have appeared to influence the work reported in this paper.

Appendix A. Supplementary material

Supplementary data to this article can be found online at https://doi.org/10.1016/j.engfailanal.2019.104361.

References

[1] D. Radaj, M. Vormwald, Advanced methods of fatigue assessment, 2013. https://doi.org/10.1007/978-3-642-30740-9.
[2] D. Radaj, C.M. Sonsino, W. Fricke, Fatigue Assessment of Welded Joints by Local Approaches: Second Edition, 2006. https://doi.org/10.1533/9781845691882.
[3] T.L. Anderson, Fracture Mechanics: Fundamentals and Applications, Third Edition -, CRC Press Book, 2005.
[4] P. Lazzarin, R. Zambardi, A finite-volume-energy based approach to predict the static and fatigue behavior of components with sharp V-shaped notches, Int. J. Fract. 112 (2001) 275–298, https://doi.org/10.1023/A:1013595930617.
[5] P. Lazzarin, R. Zambardi, The equivalent strain energy density approach re-formulated and applied to sharp V-shaped notches under localized and generalized plasticity, Fatigue Fract. Eng. Mater. Struct. 25 (2002) 917–928, https://doi.org/10.1046/j.1460-2695.2002.00543.x.
[6] P. Lazzarin, P. Livieri, F. Berto, M. Zappalorto, Local strain energy density and fatigue strength of welded joints under uniaxial and multiaxial loading, Eng. Fract. Mech. 75 (2008) 1875–1889, https://doi.org/10.1016/J.ENGFRACMECH.2006.10.019.
[7] F. Berto, P. Lazzarin, Recent developments in brittle and quasi-brittle failure assessment of engineering materials by means of local approaches, Mater. Sci. Eng. R Rep. 75 (2014) 1–48, https://doi.org/10.1016/j.mser.2013.11.001.
[8] D. Radaj, State-of-the-art review on the local strain energy density concept and its relation to the J-integral and peak stress method, Fatigue Fract. Eng. Mater.

Struct. 38 (2015) 2–28, https://doi.org/10.1111/ffe.12231.
[9] C. Fischer, W. Fricke, C.M. Rizzo, Review of the fatigue strength of welded joints based on the notch stress intensity factor and SED approaches, Int. J. Fatigue 84 (2016) 59–66, https://doi.org/10.1016/j.ijfatigue.2015.11.015.
[10] R. Negru, L. Marsavina, H. Filipescu, C. Căplescu, T. Voiconi, Assessment of brittle fracture for PUR materials using local strain energy density and theory of critical distances, Theor. Appl. Fract. Mech. 79 (2015) 62–69, https://doi.org/10.1016/j.tafmec.2015.07.011.
[11] L. Marsavina, F. Berto, R. Negru, D.A. Serban, E. Linul, An engineering approach to predict mixed mode fracture of PUR foams based on ASED and micro-mechanical modelling, Theor. Appl. Fract. Mech. 91 (2017) 148–154, https://doi.org/10.1016/j.tafmec.2017.06.008.
[12] B. Atzori, F. Berto, P. Lazzarin, M. Quaresimin, Multi-axial fatigue behaviour of a severely notched carbon steel, Int. J. Fatigue 28 (2006) 485–493, https://doi.org/10.1016/j.ijfatigue.2005.05.010.
[13] F. Berto, A criterion based on the local strain energy density for the fracture assessment of cracked and V-notched components made of incompressible hyperelastic materials, Theor. Appl. Fract. Mech. 76 (2015) 17–26, https://doi.org/10.1016/j.tafmec.2014.12.008.
[14] P. Lazzarin, C.M. Sonsino, R. Zambardi, A notch stress intensity approach to assess the multiaxial fatigue strength of welded tube-to-flange joints subjected to combined loadings, Fatigue Fract. Eng. Mater. Struct. 27 (2004) 127–140, https://doi.org/10.1111/j.1460-2695.2004.00733.x.
[15] P. Livieri, P. Lazzarin, Fatigue strength of steel and aluminium welded joints based on generalised stress intensity factors and local strain energy values, Int. J. Fract. 133 (2005) 247–276, https://doi.org/10.1007/s10704-005-4043-3.
[16] B. Atzori, P. Lazzarin, G. Meneghetti, Fatigue strength assessment of welded joints: From the integration of Paris' law to a synthesis based on the notch stress intensity factors of the uncracked geometries, Eng. Fract. Mech. 75 (2008) 364–378, https://doi.org/10.1016/j.engfracmech.2007.03.029.
[17] F. Berto, P. Lazzarin, Fatigue strength of structural components under multi-axial loading in terms of local energy density averaged on a control volume, Int. J. Fatigue 33 (2011) 1055–1065, https://doi.org/10.1016/j.ijfatigue.2010.11.019.
[18] F. Berto, A. Vinogradov, S. Filippi, Application of the strain energy density approach in comparing different design solutions for improving the fatigue strength of load carrying shear welded joints, Int. J. Fatigue 101 (2017) 371–384, https://doi.org/10.1016/j.ijfatigue.2016.09.001.
[19] S.M.J. Razavi, P. Ferro, F. Berto, J. Torgersen, Fatigue strength of blunt V-notched specimens produced by selective laser melting of Ti-6Al-4V, Theor. Appl. Fract. Mech. 97 (2018) 376–384, https://doi.org/10.1016/j.tafmec.2017.06.021.
[20] F.J. Gómez, M. Elices, F. Berto, P. Lazzarin, A generalised notch stress intensity factor for U-notched components loaded under mixed mode, Eng. Fract. Mech. 75 (2008) 4819–4833, https://doi.org/10.1016/j.engfracmech.2008.07.001.
[21] F. Berto, P. Lazzarin, A review of the volume-based strain energy density approach applied to V-notches and welded structures, Theor. Appl. Fract. Mech. 52 (2009) 183–194, https://doi.org/10.1016/j.tafmec.2009.10.001.
[22] F. Berto, P. Lazzarin, F.J. Gómez, M. Elices, Fracture assessment of U-notches under mixed mode loading: Two procedures based on the "equivalent local mode I" concept, Int. J. Fract. 148 (2007) 415–433, https://doi.org/10.1007/s10704-008-9213-7.
[23] F.J. Gómez, M. Elices, F. Berto, P. Lazzarin, Local strain energy to assess the static failure of U-notches in plates under mixed mode loading, Int. J. Fract. 145 (2007) 29–45, https://doi.org/10.1007/s10704-007-9104-3.
[24] P. Lazzarin, F. Berto, M.R. Ayatollahi, Brittle failure of inclined key-hole notches in isostatic graphite under in-plane mixed mode loading, Fatigue Fract. Eng. Mater. Struct. 36 (2013) 942–955, https://doi.org/10.1111/ffe.12057.
[25] K. Taghizadeh, F. Berto, E. Barati, Local strain energy density applied to martensitic steel plates weakened by U-notches under mixed mode loading, Theor. Appl. Fract. Mech. 59 (2012) 21–28, https://doi.org/10.1016/j.tafmec.2012.05.003.
[26] J. Justo, J. Castro, S. Cicero, Energy-based approach for fracture assessment of several rocks containing U-shaped notches through the application of the SED criterion, Int. J. Rock Mech. Min. Sci. 110 (2018) 306–315, https://doi.org/10.1016/j.ijrmms.2018.07.013.
[27] S.M.J. Razavi, P. Ferro, F. Berto, Fatigue assessment of Ti–6Al–4V circular notched specimens produced by selective laser melting, Metals (Basel) 7 (2017) 1–10, https://doi.org/10.3390/met7080291.
[28] P. Lazzarin, T. Lassen, P. Livieri, A notch stress intensity approach applied to fatigue life predictions of welded joints with different local toe geometry, Fatigue Fract. Eng. Mater. Struct. 26 (2003) 49–58, https://doi.org/10.1046/j.1460-2695.2003.00586.x.
[29] M.P. Bendsøe, Topology optimization topology optimization, in: C.A. Floudas, P.M. Pardalos (Eds.), Encycl. Optim. Springer US, Boston, MA, 2009, pp. 3928–3929 https://doi.org/10.1007/978-0-387-74759-0_685.
[30] O. Sigmund, K. Maute, Topology optimization approaches, Struct. Multidiscip. Optim. 48 (2013) 1031–1055, https://doi.org/10.1007/s00158-013-0978-6.
[31] M.L. Williams, Stress singularities resulting from various boundary conditions, J. Appl. Mech. 19 (1952) 526–528, https://doi.org/10.1115/1.321174.
[32] B. Gross, A. Mendelson, Plane elastostatic analysis of V-notched plates, Int. J. Fract. Mech. 8 (1972) 267–276, https://doi.org/10.1007/BF00186126.
[33] D. Radaj, F. Berto, P. Lazzarin, Local fatigue strength parameters for welded joints based on strain energy density with inclusion of small-size notches, Eng. Fract. Mech. 76 (2009) 1109–1130, https://doi.org/10.1016/j.engfracmech.2009.01.009.
[34] P. Lazzarin, F. Berto, Some expressions for the strain energy in a finite volume surrounding the root of blunt V-notches, Int. J. Fract. 135 (2005) 161–185, https://doi.org/10.1007/s10704-005-3943-6.
[35] P. Lazzarin, F. Berto, From Neuber's elementary volume to Kitagawa and Atzori's diagrams: An interpretation based on local energy, Int. J. Fract. 135 (2005) 33–38, https://doi.org/10.1007/s10704-005-4393-x.
[36] Z. Yosibash, A. Bussiba, I. Gilad, Failure criteria for brittle elastic materials, Int. J. Fract. 125 (2004) 307–333, https://doi.org/10.1007/978-1-4614-1508-4.
[37] P. Lazzarin, F. Berto, M. Zappalorto, Rapid calculations of notch stress intensity factors based on averaged strain energy density from coarse meshes: Theoretical bases and applications, Int. J. Fatigue 32 (2010) 1559–1567, https://doi.org/10.1016/j.ijfatigue.2010.02.017.
[38] W. Fricke, IIW guideline for the assessment of weld root fatigue, Weld. World 57 (2013) 753–791, https://doi.org/10.1007/s40194-013-0066-y.
[39] P. Lazzarin, F. Berto, F.J. Gomez, M. Zappalorto, Some advantages derived from the use of the strain energy density over a control volume in fatigue strength assessments of welded joints, Int. J. Fatigue 30 (2008) 1345–1357, https://doi.org/10.1016/j.ijfatigue.2007.10.012.
[40] C. Fischer, W. Fricke, C.M. Rizzo, Experiences and recommendations for numerical analyses of notch stress intensity factor and averaged strain energy density, Eng. Fract. Mech. 165 (2016) 98–113, https://doi.org/10.1016/j.engfracmech.2016.08.012.
[41] G. Meneghetti, A. Campagnolo, F. Berto, Averaged strain energy density estimated rapidly from the singular peak stresses by FEM: Cracked bars under mixed-mode (I + III) loading, Eng. Fract. Mech. 167 (2016) 20–33, https://doi.org/10.1016/j.engfracmech.2016.03.040.